

Nanolaminated Al₂O₃/HfO₂ dielectrics for silicon carbide based devices

Raffaella Lo Nigro^{1,a)}, Emanuela Schilirò¹⁾, Patrick Fiorenza¹⁾ and Fabrizio Roccaforte¹⁾

¹Consiglio Nazionale delle Ricerche, Istituto per la Microelettronica e Microsistemi (IMM),
Strada VIII n5, 90121 Catania, Italy

a) Electronic mail: raffaella.lonigro@imm.cnr.it

Abstract

Nanolaminated Al₂O₃/HfO₂ thin films as well as single Al₂O₃ and HfO₂ layers have been grown as gate dielectrics by Plasma Enhanced Atomic Layer Deposition (PEALD) technique on silicon carbide (4H-SiC) substrates. All the three dielectric films have been deposited at temperature as low as 250°C, with a total thickness of about 30 nm and in particular, the nanolaminated Al₂O₃/HfO₂ films have been fabricated by alternating nanometric Al₂O₃ and HfO₂ layers. The structural characteristics and dielectric properties of the nanolaminated Al₂O₃/HfO₂ films have been evaluated and compared to those of the parent Al₂O₃ and HfO₂ single layers. Moreover, the structural properties and their evolution upon annealing treatment at 800°C have been investigated as preliminary test for their possible implementation in the device fabrication flow-chart. On the basis of the collected data, the nanolaminated films demonstrated to possess promising dielectric behavior with respect to the simple oxide layers.

I. INTRODUCTION

High critical electric field, high electron mobility and high thermal conductivity are the main characteristics of the silicon carbide, which is one of the principally investigated wide band gap semiconductors for many electronics applications.¹ Among the several polymorphs of this material,² the (0001)4H-SiC substrates are the most used for their superior electronics properties and investigated in order to fabricate a new generation of power devices, whose performances are expected to go well beyond the silicon limits.³⁻⁵ From an applicative point of view, (0001)4H-SiC substrate for power device fabrication offers the possibility to form the same native oxide as in silicon (i.e., SiO₂), which can be used as gate insulator in metal-oxide-semiconductor field-effect transistors (MOSFETs).⁶ However, considering the permittivity values of both 4H-SiC substrate and SiO₂ insulator (9.7 and 3.9, respectively), the electric field in the gate oxide of a 4H-SiC MOSFET is typically a factor of 2.5 higher than in the 4H-SiC drift layer.¹ In this context, high permittivity (high- κ) insulators could allow to overcome this limitation, enabling a better redistribution of the electric field between insulator and SiC and guaranteeing safer operation conditions for the insulator in high voltage applications.

Aluminum oxide (Al₂O₃) thin films are the most studied high- κ dielectrics, due to the good insulating properties and to its thermal and chemical stability. In particular, the dielectric constant value ($\kappa \sim 9$), the relatively large band gap (~ 9 eV) and the high critical electric field (10 MV/cm) make the Al₂O₃ material a promising high- κ oxide, suitable to replace the traditional SiO₂ dielectric in several microelectronics devices.⁷⁻⁹ On the other hand, hafnium oxide (HfO₂) has been also extensively studied as a potential alternative to

silicon oxide SiO₂ especially due to its quite high dielectric constant, ($\kappa \sim 20$), while the principal HfO₂ drawback is related to its not so wide band gap (5.7 eV).¹⁰

Hence, it is clear that the selection of a dielectric for gate insulation in wide band gap semiconductors based devices, is not straightforward, but many issues need to be considered, such as the dielectric constant, bandgap and band alignment, breakdown field, mechanical and thermal stability.¹¹⁻¹⁵ As an example, to reduce the leakage current through the dielectric, the barrier height must be sufficiently high in combination with the high dielectric constant. In this context, the choice of the Al₂O₃/HfO₂ system is motivated by the possibility to combine the complementary characteristics of the two materials, i. e. the Al₂O₃ excellent chemical and thermal stability, large band gap (around 9 eV) and the HfO₂ high dielectric constant. Therefore, their nanolaminated structure composed of the two high-k oxides is a promising solution for enhancing thermal stability and sustain a high dielectric constant value.¹⁶ Several nanolaminated structures have attracted great attention for the possibility of tuning their mechanical or physical properties and have been applied in differently specific applications.¹⁷ However, in microelectronics,^{18,19} the Al₂O₃-HfO₂ nanolaminated films seem to be the most promising system and they have been mainly studied to be used for silicon based microelectronics²⁰⁻²⁴ as well as in gallium nitride power electronics devices.²⁵⁻²⁹ Poor literature is present on the study of nanolaminated systems on silicon carbide substrate. In particular, to our best knowledge only evaluation of an Y₂O₃/Al₂O₃ multilayer³⁰ and of a simple Al₂O₃/HfO₂ bilayer³¹ have been reported.

In this paper, the growth via Plasma Enhanced Atomic Layer Deposition (PEALD) of nanolaminated Al₂O₃-HfO₂ multilayers has been implemented on (0001) 4H-SiC

substrates at low deposition temperature of 250°C. The implementation of ALD on 4H-SiC substrates

is related to the peculiarities of the deposition mechanism. In particular, because of the self-limiting principle and of the layer-by-layer growth mode, ALD guarantees the conformal and uniform film deposition on large area, with precise thickness control at relatively low deposition temperatures.³² The described ALD features play a fundamental role in several new generation industrial fields.

The structural properties of the Al₂O₃/HfO₂ nanolaminated layers have been investigated and compared to those of the analogously grown Al₂O₃ and HfO₂ single layers. The study of the possible advantages of nanolaminated system with respect to the single oxides films has been completed by evaluation of their thermal stability upon post deposition high temperature annealings as well as of their dielectric properties.

II. EXPERIMENTAL

Trimethylaluminum (TMA) and tetrakis- dimethylamino hafnium (TDMAH) have been used to deposit Al₂O₃ and HfO₂ films, respectively. These metal precursors were purchased by Air Liquid as bubblers. The TMA was used at room temperature, since it is a liquid precursor, while the hafnium precursor is a solid at room temperature, and it needed to be heated at 75°C.³³ A nitrogen flow of 40 sccm was used as carrier gas to deliver the TMA and TDMAH from the bubbler to the reactor chamber. Depositions were carried out on a 5 nm thermally grown SiO₂ layer formed on (0001) 4H-SiC substrates. Prior to SiO₂ thermal growth, the 4H-SiC wafers were treated with piranha solution (H₂SO₄:H₂O₂=1:3 for 10 min) and with diluted hydrofluoric acid (H₂O:HF=10:1 for 5

min) to remove and to clean the surface from carbon contaminations and eventual impurities. After these cleaning treatments, the 4H-SiC substrates were subjected to a controlled dry oxidation process at 1150°C in dry O₂-atmosphere to grow a 5 nm thick SiO₂ layer.³⁴

Film deposition parameters

Films were deposited on PE ALD LL SENTECH Instruments GmbH reactor. The ALD system is equipped with a remote capacitively coupled plasma (CCP) source. It is excited by a 13.56 MHz RF generator via a matchbox. The power supply was 200 W and the oxygen-gas-flow-rate was 150 sccm.

Depositions were carried out at 250°C with a reactor chamber pressure of 20 Pa. For the Al₂O₃ deposition, the pulse times of metal precursor and oxygen pulse were 0.06s and 1s, respectively. For the HfO₂ deposition, the pulse times of metal precursor and oxygen pulse were 0.1s and 5s, respectively. After each precursor pulse, the deposition chamber was purged with 40 sccm N₂ to remove un-reacted precursors.

The Al₂O₃/HfO₂ nanolaminated films were deposited by repeating a unit cycle for precise thickness control. In particular, the Al₂O₃/HfO₂ nanolaminated film consisted of twenty total nanolayers. Each Al₂O₃ or HfO₂ nanolayer has been obtained by five unit cycles, with a unit cycle comprising a precursor, purge, oxygen reactant and final purge.

The deposited nanolaminated films were annealed by rapid thermal annealing process, which was carried out at 800°C in N₂ atmosphere for 1 minute in a Jetfirst 150 JIPELEC furnace.

Structural and Morphological Characterizations

Microstructures were investigated by transmission electron microscopy (TEM) using a FEG-TEM JEOL 2010F. Morphological characterization was performed by atomic force microscopy (AFM), which was carried out on a Digital Instrument D3100 operating in air.

Device fabrications

The test-patterns for the electrical characterization were fabricated using top Ni/Au electrodes. On the deposited films, Ni/Au bilayer, consisting of 80 nm of each metal, were deposited by sputtering and patterned by standard optical lithography and lift-off technique, to fabricate circular diodes.

The dielectric constants were determined by capacitance voltage (C/V) measurements, which were carried out using a Karl-Suss probe station equipped with an Agilent B1500A parameter analyzer.

III. RESULTS AND DISCUSSION

Laminated Al₂O₃/HfO₂ thin films as well as single Al₂O₃ and HfO₂ layers have been deposited by plasma enhanced atomic layer deposition (PE-ALD) processes. Simple oxide Al₂O₃ and HfO₂ layers have been considered as references to compare the physical properties of their combination as laminated stack. Some of the deposition parameters, which have been used for the growth of the two different films, possess common values and in particular they consisted in deposition temperature of 250°C, 200 W plasma

power, 40 sccm nitrogen gas carrier for the two metal precursors and total deposition pressure of 20 Pascal. The other parameters, which needed to be different for the growth of the two Al₂O₃ and HfO₂ layers have been reported on Table 1.

Table 1. Specific deposition parameters for the growth of Al₂O₃ and HfO₂ thin films

Film	Metal Precursor Pulse/Purge	O ₂ Plasma Pulse/Purge	Number of Cycles
Al ₂ O ₃	0.06s/2s	1s/2s	250
HfO ₂	0.1/5s	5s/2s	100

Both growth processes have not been carried out on the bare (0001) 4H-SiC substrate but on a 5 nm thermally grown SiO₂ layer, which have been formed on its surface. This strategy has been proven to be the most useful in order to deposit quite dense and compact films, because of the presence of a greater number of active sites for nucleation with respect to the bare surface of the silicon carbide.³⁴ The growth rates of the Al₂O₃ and HfO₂ processes have been evaluated to be 1.1 Å/cycle and 1.6 Å/cycle, respectively. The indicated growth rate values have been calculated using the deposition parameters showed on table 1. In our previous papers,^{16,34,35} the growth rates of the two different Al₂O₃ and HfO₂ layers grown on silicon substrate have been determined by evaluation of film thickness through ellipsometric measurements and corroboration of the thickness value by TEM imaging. An accurate evaluation of the growth rates was carried out by plotting the growth rate vs the number of cycles and linear trends were found in both cases. In this work, the growth rates have been determined by TEM analysis and they are in agreement with those found for Al₂O₃ and HfO₂ PE-ALD processes on silicon

substrate. Cross-section TEM images (Fig. 1) have been recorded to also investigate the structural properties of the two Al_2O_3 and HfO_2 single layers. In particular, Al_2O_3 as-deposited film possesses a uniform thickness of about 30 nm, it is amorphous and adherent to $\text{SiO}_2/4\text{H-SiC}$ substrate. On the other hand, the HfO_2 layer, deposited using 100 cycles as shown on table 1, demonstrated to have a lower thickness value of 14-16 nm and despite the amorphous nature of the initial 10-12 nm layer, some small grains are visible on the film surface. The formation of crystalline grains is an already known phenomenon reported literature,³⁵ generating a polycrystalline structure beyond a critical thickness of about 10 nm.

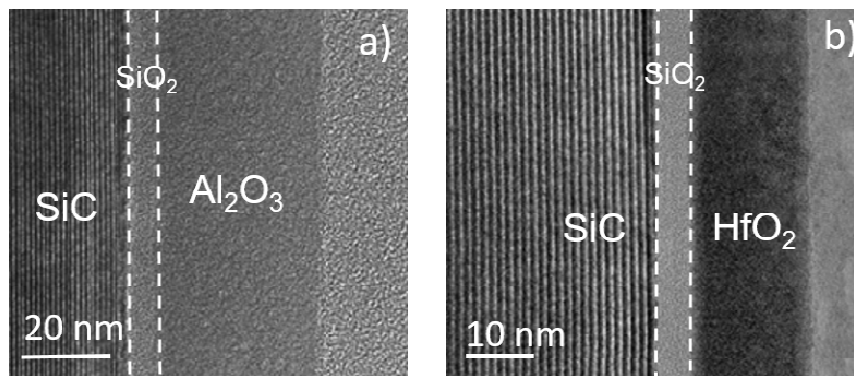


Fig. 1. TEM cross-section images of Al_2O_3 (a) and HfO_2 (b) thin films grown by PEALD on $\text{SiO}_2/(0001)$ SiC substrates.

AFM characterization has been carried out to investigate the superficial morphology of the deposited film. In particular, $1\mu\text{m}\times 1\mu\text{m}$ areas have been imaged and the relative AFM bidimensional maps are shown Fig. 2 and compared to the substrate morphology (Fig. 2a). Film morphologies are characterized by smooth surfaces but also the presence of small circular grains is evident (Fig.s 2b and 2c). Their calculated root mean square (RMS) values, namely 0.56 nm and 0.61 nm, for Al_2O_3 and HfO_2 thin films, respectively,

demonstrated that films are slightly rougher than the bare silicon carbide substrate (0.26 nm).

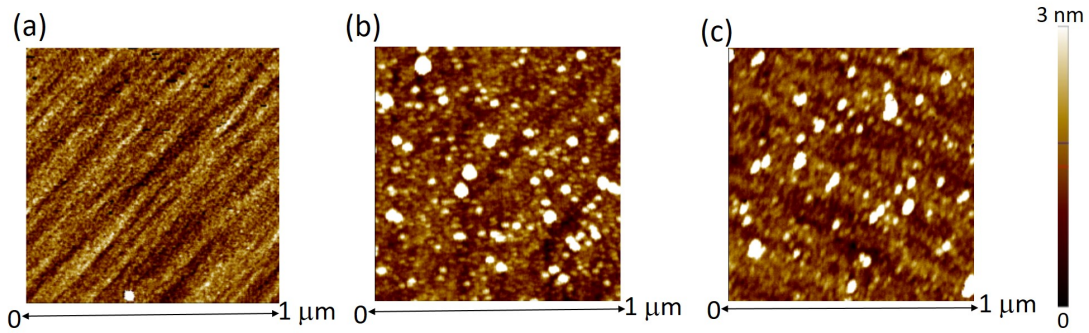


FIG. 2. AFM bidimensional maps of the SiO₂/4H-SiC substrate (a), Al₂O₃ (b) and HfO₂ (c) thin films grown by PEALD processes.

Finally, the dielectric properties of the two Al₂O₃ and HfO₂ films have been studied by the capacitance-voltage (*C/V*) measurements. The *C/V* curves (Fig. 3) of the two samples have been recorded on test-patterns which have been fabricated by several steps. *C/V* measurements have been performed at 1 MHz and the accumulation capacitances have been used to calculate the dielectric constant values. The dielectric constant value of the Al₂O₃ is 8.2, while in the case of HfO₂ films has been evaluated to be about 10.

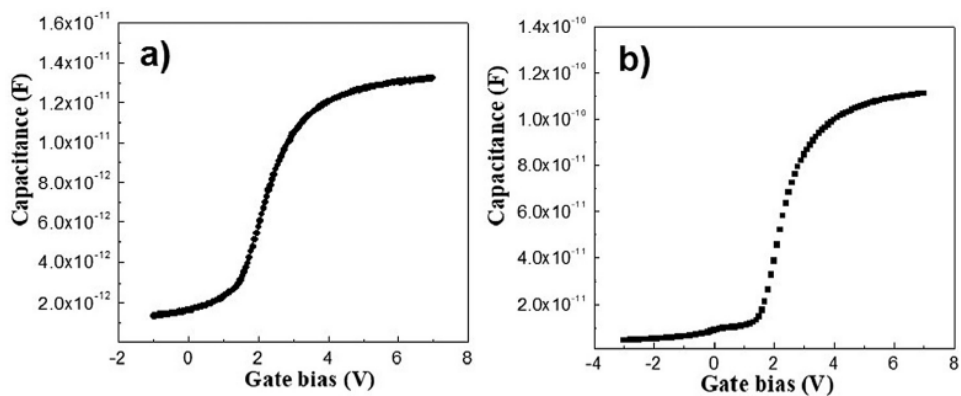


FIG. 3. *C/V* curves recorded at 1 MHz for Al₂O₃ (a) and HfO₂ (b) films deposited by PEALD processes.

The comparison of the characterization data between the two deposited films suggests a better thermal stability of the Al₂O₃ film with respect to that of HfO₂ layer, while this last possesses a higher dielectric constant value. The results are in agreement with the predicted behavior from the literature data³⁶ and their combination as laminated system has been considered in order to get the improved performances.

The proposed laminated system is schematically shown in Fig 4a and it consists of a 10 stacked Al₂O₃/HfO₂ bilayer, with each single oxide sub-layer having a thickness minor than 2 nm. The nanolaminated film has been fabricated using the same values of the main deposition parameters which have been described for the growth of the single layers, i. e. deposition temperature, process pressure and plasma value, while the cycles sequence has been appropriately modified. In particular, the two precursors have been alternatively pulsed into the reactor chamber and an extended purge time has been optimized in order to clean from the residual precursors both the substrate surface and the entire chamber, thus avoiding cross contamination between the different precursors.

The formation of the desired nanolaminated film has been demonstrated by TEM analysis, in fact, as shown in Fig 4c the formation of a laminated structure having sharp interfaces is clearly visible. The total film thickness is 36 nm and each sublayer is about 1.8 nm. The growth rate in the case of the nanolaminated film is about 1.2 Å/cycle and it is quite similar to the values of the processes for the growth of simple Al₂O₃ and HfO₂ oxides. In this context, it should be noted that in the TEM image, the thickness of the HfO₂ sub-layer seems to possess a slightly higher value than that of the Al₂O₃, however, this mis-interpretation could be due to the intrinsically darkest mass contrast of the HfO₂ with respect to the Al₂O₃ ones. An annealing treatment, at 800°C in N₂ atmosphere, has

been performed on the laminated sample in order to check the thermal stability of the fabricated stack. The relative TEM image (Fig 4d) after the thermal treatment showed that it resulted in a small decrease (about 2 nm) of the total thickness, probably because of a densification process. In addition, the interfaces between the sub-layers became less sharp and diffusive phenomena, activated by high temperature, favored a light intermixing process between Al_2O_3 and HfO_2 nanolayers. Nevertheless, no structural evolution occurred upon the performed annealing process, in fact, no evident crystallization appeared as demonstrated by the electron diffraction pattern which did not show any diffraction spot except those from the substrate (not shown).

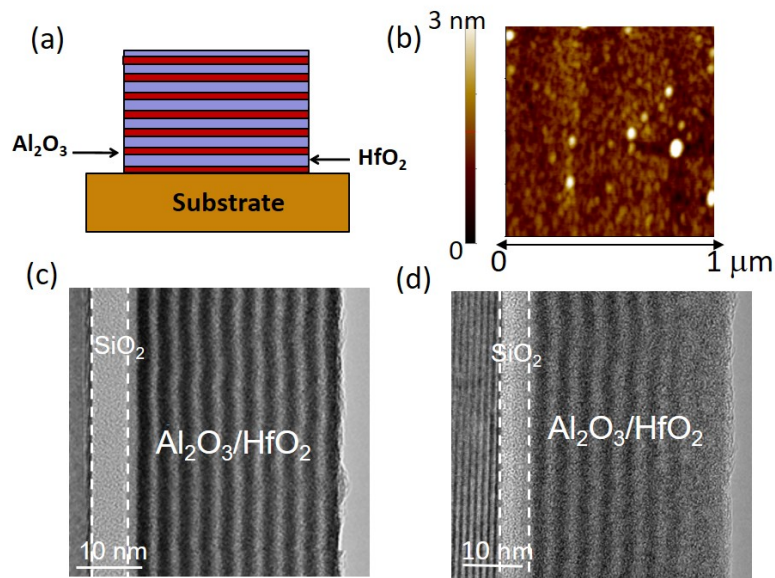


FIG. 4. Schematic of the $\text{Al}_2\text{O}_3/\text{HfO}_2$ laminated film (a) and its AFM bidimensional map (b). The cross section TEM image (c) shows the formation of about 1.8 nm alternating Al_2O_3 and HfO_2 thin layers in the as-dep film, whose interfaces became not so defined after annealing, as shown in the TEM image (d) recorded after the 800°C treatment.

This information on the amorphous nature of the annealed nanolaminated films represents an important result showing that the missed crystallization process, upon annealing at temperature well beyond the HfO₂ crystallization value (500°C), is a promising solution to improve the thermal stability of the nanolaminated dielectric.

In addition to the studies on the structural properties, the morphological characterization has been performed using AFM investigation. AFM mapping pointed out to a quite smooth surface and a morphology characterized by rounded grains, with root mean square of the height distribution value of 0.58 nm, quite similar to the values found in the single Al₂O₃ and HfO₂ single layers. Similar morphology as well as RMS value have been observed on the annealed samples.

A detailed electrical characterization of both as-deposited and annealed laminated samples has been performed by the capacitance voltage (C/V) curves, which have been reported in Fig 5. In particular, a more extensive study of the dielectrical properties has been carried out by evaluation of the shape and the position of the C-V characteristics which are directly related to the amount of charged defects in the insulator and at the insulator/semiconductor interface.

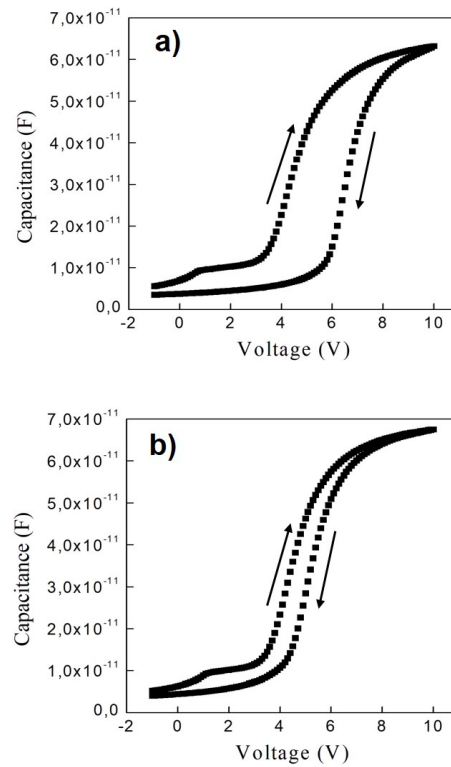


FIG. 5. C-V curves, recorded at 1 MHz, of Al₂O₃/HfO₂ nanolaminated films as-deposited by PE-ALD (a) and after annealing process at 800°C in N₂ atmosphere (b).

Hence, the C/V curves have been recorded at 1 MHz from depletion to accumulation and backwards, and have been used to experimentally determine not only the dielectric constant values but other dielectric parameters, such as the flat band voltage which is related to the number of charged defects and the hysteresis which is associated with the number of trapped (negative) charges.

The dielectric constant value of the as-deposited laminated film has been calculated to be 12.4.

The unbalanced charges arising from defects cause a C/V curve shift moving the flat band voltage from the ideal condition. In the case of Ni based contacts, the ideal flat band

voltage value has been calculated to be $V_{FB\ Theor} = 1.28V$. The shift value between the theoretical ($V_{FBTheor}$) and experimental (V_{FB}) can be used to quantify the number of fixed charges (N_f [cm^{-2}]) in the dielectric film using the equation:

$$N_f = \frac{C_{ox}\Delta V_{FB}}{eA}$$

where C_{ox} is the accumulation capacitance, e is the elementary electron charge, A is the area of the gate and ΔV_{FB} is the flat band shift.

In addition, by the flat band shift between the backward and forward C-V curves (hysteresis), the oxide trapping states (N_{ot}) can be quantified.

The estimated N_f and N_{ot} values are $N_f = 4 \times 10^{12} \text{ cm}^{-2}$ and $N_{ot} = 2.7 \times 10^{12} \text{ cm}^{-2}$, respectively.

After the annealing treatment at $800^\circ C$ in N_2 , the laminated stack showed an improvement of the dielectric properties. In fact, both the dielectric constant value improved to 13.4 and the Q_{ot} value decreased to $1.15 \times 10^{12} \text{ cm}^{-2}$. The increasing of the dielectric constant value could be associated with the densification process already discussed and showed in the TEM image (Fig 4d), as well as it could be related to the probable formation of some single $HfAlOx$ phase due to the light intermixing observed at the nanolayer interfaces.

All these results indicated a quite good insulating behavior of the laminated stack. Moreover, also the comparison of the complete structural and dielectric data of single Al_2O_3 or HfO_2 and their laminated combination, pointed out that the nanolaminated can be considered a promising system. In fact, it showed an amorphous structure before and after the annealing treatment and a better dielectric behavior in terms of dielectric constant and charge traps amounts. Further improvement of the dielectric properties

could be achieved by changing the $\text{Al}_2\text{O}_3/\text{HfO}_2$ ratio. In particular, maintaining constant the total film thickness and the number of alternating layer, while changing the Al_2O_3 and HfO_2 nanolayer thicknesses, i.e. the HfO_2 thickness could be increased while the Al_2O_3 ones could be decreased. This strategy will be evaluated for our future experiments.

IV. SUMMARY AND CONCLUSIONS

Huge efforts are nowadays devoted to the fabrication of multicomponent systems having high dielectric constants and good chemical stability. In particular, Al_2O_3 and HfO_2 oxides might be combined on the basis of their intrinsic physical properties. Three dielectric layers, namely Al_2O_3 , HfO_2 and $\text{Al}_2\text{O}_3/\text{HfO}_2$ laminated, have been deposited on silicon carbide substrates by PEALD with the same thickness and their thermal stability and dielectric properties have been compared. The Al_2O_3 layer possesses good thermal stability but low dielectric constant. The HfO_2 layer possesses the higher dielectric constant value (about 10) but low thermal stability and as a consequence highest leakage current density and lowest reliability, while the combination of aluminum oxide and hafnium oxide in nanolaminated system improved the relatively low thermal stability of HfO_2 ($\sim 500^\circ\text{C}$) and increased the relatively low dielectric constant (~ 13) of Al_2O_3 thin films.

ACKNOWLEDGMENTS

This work was funded by the European Community in the framework of the ECSEL Research and Innovation Actions (RIA) Calls 2016, Project WInSiC4AP (Wide band gap Innovative SiC for Advanced Power), Project Number: [737483]

REFERENCES

- ¹ B. J. Baliga, *Silicon Carbide Power Devices* (World Scientific Publishing Co. Pte. Ltd., Singapore, 2005)
- ² J. Kelly, G. R. Fisher, and P. Barnes, *Mater. Res. Bull.* **40**, 249 (2007)
- ³ T. Kimoto, *Jap. J. Appl. Phys.* **54**, 040103 (2015)
- ⁴ F. Roccaforte, P. Fiorenza, G. Greco, M. Vivona, R. Lo Nigro, F. Giannazzo, A. Patti and M. Saggio, *Appl. Surf. Sci.* **301**, 9 (2014)
- ⁵ G. Liu, B. R. Tuttle, and S. Dhar, *Appl. Phys. Rev.* **2**, 021307 (2015)
- ⁶ F. Roccaforte, P. Fiorenza, G. Greco, R. Lo Nigro, F. Giannazzo, F. Iucolano and M. Saggio, *Microelec. Eng.* **187-188**, 66 (2018)
- ⁷ F. Zhang, G. Sun, L. Zheng, S. Liu, B. Liu, L. Dong, L. Wang, W. Zhao, X. Liu, G. Yan, L. Tian and Y. Zen, *J. Appl Phys* **113**, 044112 (2013)
- ⁸ M. Avice, U. Grossner, I. Pintlilie, B. G. Svensson, M. Servidori, R. Nipoti, O. Nilsen and H. Fjellvåg, *J. Appl. Phys.* **102**, 054513 (2007)
- ⁹ H. Moriya, S. Hino, N. Miura, T. Oomori and E. Tokumitsu, *Mater. Sci. Forum.* **615-617**, 777 (2009)
- ¹⁰ G. D. Wilk, R. M. Wallace and J. M. Anthony, *J. Appl. Phys.* **89**, 5243 (2001).
- ¹¹ R. K. Chanana, K. McDonald, M. Di Ventura, S. T. Pantelides, L. C. Feldman, G. Y. Chung, C. C. Tin, J. R. Williams, and R. A. Weller, *Appl. Phys. Lett.* **77**, 2560 (2000)
- ¹² P. Fiorenza, A. Frazzetto, A. Guarnera, M. Saggio and F. Roccaforte, *Appl. Phys. Lett.* **105**, 142108 (2014)
- ¹³ J. Robertson *J. Vac. Sci. Technol. B* **18**, 1785 (2000)
- ¹⁴ F. Roccaforte, P. Fiorenza, G. Greco, R. Lo Nigro, F. Giannazzo, A. Patti and M. Saggio, *Phys. Status Solidi A* **211**, 2063 (2014)
- ¹⁵ R. Singh, *Microelectron. Reliab.* **46**, 713 (2006).
- ¹⁶ R. Lo Nigro, E. Schilirò, G. Greco, P. Fiorenza and F. Roccaforte, *Thin Solid Films* **601**, 68 (2016).
- ¹⁷ M. Knez, K. Nielsch and K. L. Niinisto, *Adv. Mater.* **19**, 3425 (2007).
- ¹⁸ H. Zhang, R. Solanki, B. Roberds, G. Bai and I. Banerjee, *J. Appl. Phys.* **87**, 1921 (2000).
- ¹⁹ K. Kukli, M. Ritala and M. Leskela, *J. Electrochem. Soc.* **148**, F35 (2001).
- ²⁰ M.-H. Cho, Y. S. Roh, C. N. Whang, K. Jeon, H. J. Choi, S. W. Nam, D.-H. Ko, J. H. Lee, N. I. Lee and K. Fujihara, *Appl. Phys. Lett.* **81**, 1071 (2002).
- ²¹ H. S. Chang, H. Hwang, M.-H. Cho, D. W. Moon, S.Y.J. Doh, J.H. Lee and N. I. Lee, *Appl. Phys. Lett.* **84**, 28 (2004).
- ²² H. Jin, S. K. Oh, H. J. Kang, S. W. Lee, Y. S. Lee and K. J. Lim, *J. Korean Phys. Soc.* **46**, S52 (2005).
- ²³ H. Jin, H. J. Kang, S. W. Lee, Y. S. Lee, S. K. Rha, H. S. Lee and K. J. Lim, *J. Korean Phys. Soc.* **45**, 1292 (2004).
- ²⁴ P. K. Park, E.-S. Cha and S. W. Kang, *Appl. Phys Lett.* **90**, 232906 (2007)
- ²⁵ P. K. Park, H.-I. Cho, H. C. Choi, Y.-H. Bae, C.-S. Lee, J.-L. Lee and J.-H. Lee, *Jap. J. Appl. Phys.* **43**, L1433 (2004).
- ²⁶ Y. Yue, Y. Hao, J. Zhang, J. Ni, W. Nao, O. Feng and L. Liu, *IEEE Electron Device Lett.* **29**, 838 (2008).
- ²⁷ C. Kirkpatrick, B. Lee, X. Yang and V. Misra, *Phys. Status Solidi C*, **7-8**, 2445 (2011).

- ²⁸B. Lee, Y. H. Choi, C. Kirkpatrick, A. O. Huang and V. Misra, *Semicond. Sci Tech.* **28**, 074016 (2013).
- ²⁹R. Suri, C. J. Kirkpatrick, D. J.; Lichtenwalner and V. Misra, *Appl. Phys. Lett.* **96**, 042903 (2010).
- ³⁰F. Zhao, O. Amnuayphol and K.-Y. Cheong, *Mater. Lett.* **245**, 174 (2019)
- ³¹M. Usman, C. Henkel and A. Hallen, *J. Solid State Sci. Tech.* **2**, N308 (2013).
- ³²R. Foest, M Schmidt, H. Gargouri, *Eur. Phys. J. D* **68**, 23 (2014)
- ³³R. Lo Nigro, E. Schilirò, C. Tudisco, G. G. Condorelli, P. Fiorenza, H. Gargouri and F. Roccaforte, *Nanotechnology Materials and Devices Conference IEEE 9th*, 112 (2014)
- ³⁴E. Schilirò, R. Lo Nigro, P. Fiorenza and F. Roccaforte, *AIP Adv.* **6**, 075201 (2016)
- ³⁵R. Lo Nigro, E. Schilirò, G. Mannino, S. Di Franco and F. Roccaforte, *J. Cryst. Growth*, in press.
- ³⁶X.-Y. Zhang, C.-H. Hsu, Y.-S. Cho, S. Zhang, S.-Y. Lien, W.-Z. Zhu and F.-B. Xiong, *Thin Solid Films* **660**, 797 (2018)
- ³⁷M. Ritala, M. Leskela, M. Niinisto, T. Prohaska, G. Friedbacher and M. Grasserbauer, *Thin Solid Films*, **72**, 250 (1994).